Bioactivities of Natural Products

Phylloxanthobilins are Abundant Linear Tetrapyrroles from Chlorophyll Breakdown with Activities Against Cancer Cells

Cornelia A. Karg,[a] Pengyu Wang,[a] Florian Kluibenschedl,[b] Thomas Müller,[b] Lars Allmendinger,[c] Angelika M. Vollmar,[a] and Simone Moser*[a]

Abstract: Linear tetrapyrroles, called phyllobilins, are obtained as major catabolites upon chlorophyll degradation. Primarily, colorless phylloleucobilins featuring four deconjugated pyrrole units were identified. Their yellow counterparts, phylloxanthobilins, were discovered more recently. Although the two catabolites differ only by one double bond, physicochemical properties are very distinct. Moreover, the presence of the double bond seems to enhance physiologically relevant bioactivities: in contrast to phylloleucobilin, we identified a potent anti-proliferative activity for a phylloxanthobilin, and show that this natural product induces apoptotic cell death and a cell cycle arrest in cancer cells. Interestingly, upon modifying inactive phylloleucobilin by esterification, an anti-proliferative activity can be observed that increases with the chain lengths of the alkyl esters. We provide first evidence for anti-cancer activity of phyllobilins, report a novel plant source for a phylloxanthobilin, and by using paper spray MS, show that these bioactive yellow chlorophyll catabolites are more prevalent in Nature than previously assumed.

Introduction

Despite its visibility, the biochemical degradation of the green plant pigment chlorophyll (Chl) has remained unresolved for a long time, until abundant linear tetrapyrroles, now called phyllobilins (PBs), were discovered as stable degradation products accumulating in the vacuoles of the plant cell.[1] In the meantime, Chl breakdown has revealed many of its mysteries, and we now have a well-defined picture of the biochemical program of Chl breakdown, called pheophorbide a oxygenase (PaO)/phyllobilin pathway. The most commonly identified "final" breakdown product is a 3^2-hydroxylated phylloleucobilin (PleB), 3^2-OH-PleB. Colorless PleBs were the first PBs to be discovered and were believed to represent the "last stage" of Chl breakdown.

For the plant *Cercidiphyllum japonicum*, in addition to 3^2-OH-PleB (*Cj*-PleB (**1**)),[2] a yellow colored oxidation product, a phylloxanthobilin (*Cj*-PxB (**2**)), was discovered for the first time 10 years ago[3] (Scheme 1).

The formation of PxBs in plants has not yet been fully clarified, but it is assumed that plants with PxB content show an endogenous "oxidative activity", likely caused by enzymes.[4] In contrast to PleBs, PxBs feature a double bond system extending from ring C to ring D, resulting not only in an intense yellow color, but also in interesting chemical properties. PxBs were shown to be reversible photoswitches and to dimerize depending on the lipophilicity of the environment in a formal [2+2] cycloaddition.[5]

Chl breakdown has been and still is regarded primarily as a detoxification process; the discovery of the PxBs, however, points towards yet to be elucidated physiological roles of these metabolites for the plant. Up to the stage of the PleBs, the efforts of the PaO/phyllobilin pathway, using metabolic energy and specific enzymes to detoxify photoactive Chl, yields non-photoactive, more water-soluble molecules with four isolated tetrapyrrole units. The discovery of PxBs, however, contradicts the detoxification paradigm. PxBs were found to be photoactive compounds[5] and are, compared to PleBs, less hydrophilic, seemingly reverting the efforts of the detoxification pathway and raising the question of a potential relevance of PxBs in physiological roles for the plant.

For humans, PxBs are suspected to have yet un-identified bioactivities, too.[6] We could recently show that the PxBs from *Echinacea purpurea* have a very potent in vitro antioxidative activity, a high radical scavenging potential in human cells, and can protect the cells from oxidative stress. Furthermore, metabolic studies indicated the PxBs to be stable in the cell.[7] An-
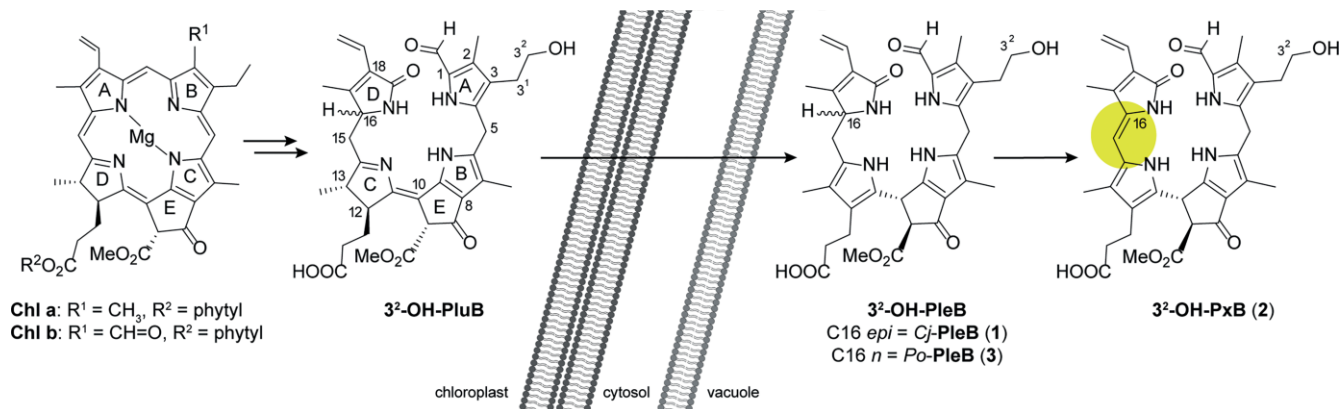
[a] C. A. Karg, P. Wang, Prof. Dr. A. M. Vollmar, Dr. S. Moser
Pharmaceutical Biology, Pharmacy Department, Ludwig-Maximilians University of Munich,
Butenandtstraße 5-13, 81377 Munich, Germany
E-mail: simone.moser@cup.uni-muenchen.de
https://www.pharmbiol.cup.uni-muenchen.de/staff/group-leaders/moser1/
[b] F. Kluibenschedl, Assoz. Prof. Dr. T. Müller
Institute of Organic Chemistry, University of Innsbruck,
Innrain 80-82, 6020 Innsbruck, Austria
[c] L. Allmendinger
Pharmaceutical Chemistry, Pharmacy Department, Ludwig-Maximilians University of Munich,
Butenandtstraße 5-13, 81377 Munich, Germany

Chl a: R[1] = CH[3], R[2] = phytyl
Chl b: R[1] = CH=O, R[2] = phytyl

3²-OH-PluB

3²-OH-PleB
C16 *epi* = *Cj*-**PleB** (1)
C16 *n* = *Po*-**PleB** (3)

3²-OH-PxB (2)

chloroplast   cytosol   vacuole

Scheme 1. Overview on key structures of chlorophyll catabolism leading - via a transient 3²-phyllolumibilin (3²-OH-PluB) – to the most commonly identified 3²-hydroxylated phylloleucobilin (3²-OH-PleB). While the absolute configuration at the stereocenter at C16 of PluBs and PleBs is not known, these catabolites can be classified as either n or epi, depending on the plant species. 3²-OH-PleB accumulates in the vacuoles; oxidation of the 3²-OH-PleB leads to the colored 3²-hydroxylated phylloxanthobilin (3²-OH-PxB (**2**)).

other PxB was isolated from de-greened leaves of savoy cabbage, which is thought to exert its health promoting effects via antioxidants. Also for this PxB, its potent in vitro antioxidative activity was proven by two different approaches.[8]

Cornelia A. Karg studied pharmacy at the Ludwig-Maximilians-University of Munich and received her approbation in pharmacy in 2017. She then started her PhD under the supervision of Prof. Angelika Vollmar and Dr. Simone Moser at the Department of Pharmaceutical Biology at the LMU. Her research topics include the structural characterization of natural products in plants and investigations on their bioactivities and molecular mode of action in cells.

Pengyu Wang received his Master's degree in Pharmaceutical Chemistry from Wuhan University, China in 2018. He then pursued his PhD degree under the guidance of Prof. Angelika Vollmar and Dr. Simone Moser at Ludwig-Maximilians-University, Munich, Germany. His research mainly focuses on discovery, modification and bioactivity evaluation of natural products from plants.

Florian Kluibenschedl is studying chemistry and physics at the University of Innsbruck, Austria. He discovered his interest in mass spectrometry in the course of two internships at the Institute of Organic Chemistry, University of Innsbruck. It was then when he performed Leaf Spray mass spectrometry experiments. He now is pursuing his bachelor thesis as a member of the Müller research group.

Thomas Müller is an Associate Professor at the Institute of Organic Chemistry, University of Innsbruck, Austria. He obtained his PhD at the Medical University of Innsbruck. During his post-doctoral period with Prof. Bernhard Kräutler (University of Innsbruck) he worked on structure elucidation of natural products isolated from plants. As a visiting scientist at Prof. R. Graham Cooks' lab (Purdue University, West Lafayette, IN, USA), he started to focus on ambient ionization techniques. The utilization of ambient ionization for structure elucidation and imaging mass spectrometry is still his main research interest.

Lars Allmendinger received his PhD degree in 2004 from the Ludwig-Maximilians-University (LMU), Munich (Germany), working on the total synthesis of a natural occurring antibiotic under the supervision of Dr. Franz Paintner. He has then overtaken the management of the NMR facility belonging to the Medici nal Chemistry unit of the Department of the LMU. In April 2020 he joined the research group of Prof Ivan Huc at the LMU in order to seek new challenges in the field of Chemical Biology.

Angelika M. Vollmar is Dean of the Faculty of Chemistry and Pharmacy and full professor at the Ludwig-Maximilians-University of Munich. She obtained her doctorate in pharmaceutical biology in 1984. After a post-doctoral stay at UCLA, USA (1985–1987), she habilitated in clinical pharmacology and pharmacy at the Faculty of Veterinary Medicine at LMU Munich in 1991. In 1991, she has been visiting researcher at the Clinical Research Institute, Montreal, followed by a professorship in pharmacology in 1994. Since 1998, she has held the Chair of Pharmaceutical Biology in the Department of Pharmacy at LMU Munich. Her research activities are in the field of drug development and focus on natural compounds as tools and leads in cancer biology and therapy. In addition to various scientific awards, she received the Federal Cross of Merit on Ribbon of Germany in 2011.

Simone Moser studied chemistry at the University of Innsbruck, Austria. She pursued doctoral studies with Prof. Kräutler at the Institute of Organic Chemistry (Innsbruck), working on structure elucidation of natural products. After postdoctoral studies as a Marie-Curie postdoctoral fellow in the group of Prof. Johnsson at EPFL, Switzerland and as Swiss National Science Foundation Fellow at MIT, USA with Prof. Nolan, she returned to Austria and worked in the pharmaceutical industry (Novartis). After a short stay at her alma mater, she moved to Munich and is currently leading a research group at LMU, working on bioactivities of natural products.

EurJOC
European Journal of Organic Chemistry

Full Paper
doi.org/10.1002/ejoc.202000692

Chemistry
Europe
European Chemical
Societies Publishing

Since PxBs appear to be overlooked bioactive constituents of plants, and compounds with structures related to PBs, such as bilirubin, have a reported anti-cancer activity,[9] we set out to test the cytotoxicity of PBs against cancer cells. We focused on the most common PB motif, the 3^2-hydroxylated core structure, 3^2-OH-PleB (1 and 3), and its PxB oxidation product 2. The PxB (2) showed promising cytotoxicity and apoptosis-inducing properties in bladder and breast cancer cells. The PleB precursors 1 and 3, in contrast, were revealed not to be toxic against cancer cells; we could show, however, that esterification of the propionic acid side chain by chemical synthesis led to tunable cytotoxicity, which could be partially explained by uptake studies.

Results and Discussion

Isolation and Structure Elucidation of PleB (3) and PxB (2) from Plane Tree (*Platanus occidentalis*)

The analytical HPLC analysis of a senescent plane tree leaf revealed two signals with UV spectra characteristics for phyllobilins (Figure 1, Figure S1). One signal was tentatively identified as PleB with absorption maxima at around 240 nm and 312 nm and one as a PxB featuring an additional maximum at 426 nm.[3] The *Po*-PleB (3) was isolated from 300 g of leaves as described in the experimental section, giving 50 mg of pure 3. In order to obtain large amounts of 2, the latter was synthesized from 3 via light assisted oxidation on silica gel.[10] Using the published protocol, 2 mg of the PxB (2) were obtained from 10 mg of 3. HRMS analysis of purified compounds allowed for the deduction of the molecular formulae as $C_{35}H_{41}O_8N_4$ for 3, and $C_{35}H_{39}O_8N_4$ for 2, revealing them to have an identical molecular composition as PleB (1) and PxB (2) from katsura tree leaves. PBs from katsura tree, *Cercidiphyllum japonicum*, have been thoroughly characterized by spectroscopic methods; the major PleB (1) was identified as 3^2-OH PleB.[2] Furthermore, the Z and E conformers of 3^2-OH-PxB (2) were identified.[3]
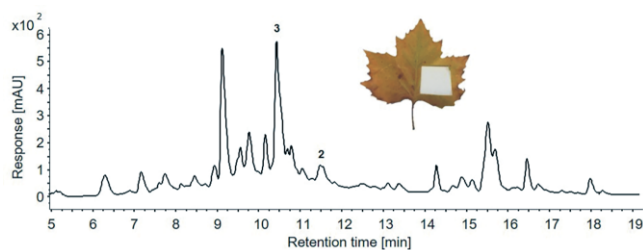

Figure 1. Analytical HPLC trace of a methanolic extract of a fresh, senescent plane tree leaf (detection at 320 nm) indicated the presence of *Po*-PleB (3) and *Po*-PxB (2).

In a co-elution experiment, in which isolated pure *Po*-PleB (3) and *Cj*-PleB (1), and a mixture of the two pure compounds, were applied to analytical HPLC, the two PleB signals showed similar but not identical retention times (Figure S2 A–C). Since the mass spectra of the two compounds revealed them to have an identical molecular formula, we conclude that the two PleBs 1 and 3 are epimers featuring a different configuration at the

stereocenter at C16. Two "classes" of PleBs, i.e. C16 epimers, result from the stereospecificity of an enzyme that introduces a new stereocenter in the PleB precursor primary phyllolumibilin (*p*PluB) either in the "*n*" or "*epi*" configuration, depending on the plant species.[11] The *p*PluB is then hydroxylated resulting in a 3^2-OH PluB, which is converted into the respective PleB by acid-induced tautomerization in the vacuoles of the senescent plant cell.[12]

The elemental composition of *Po*-PxB (2) was deduced via HRMS as $C_{35}H_{39}O_8N_4$ and revealed the structure to be identical with *Cj*-PxB (2) from katsura. A co-elution experiment was performed, in which the isolated compounds *Cj*-PxB (2), *Po*-PxB (2), and a mixture of both compounds, were analyzed by analytical HPL-chromatography. The chromatograms showed identical peaks and chromatographic characteristics (Figure S2 D–F). Moreover, these findings were confirmed by ^{1}H NMR spectroscopy. By comparing the ^{1}H NMR spectrum of *Po*-PxB (2) with the spectrum of *Cj*-PxB (2),[3] the same typical signals for a tetrapyrrolic PxB stood out: the characteristic signal pattern for the spin system of the peripheral vinyl group at the intermediate field; four singlets at high field of the methyl groups H_3C2^1, H_3C7^1, H_3C13^1, and H_3C17^1 near 2 ppm, and one singlet of the methyl ester group at 3.7 ppm. Moreover, one singlet at the low field for the formyl group was detected, as well as the characteristic signal for the additional double bond in a PxB core in Z conformation,[3] a singlet of HC15 at 6.19 ppm (Figure S5, Table S2). In conclusion, the spectroscopic data clearly show the PxB from *Platanus* to be identical to the PxB (2) from *Cercidiphyllum japonicum*.

Analysis of PBs in Senescent Leaves by Paper Spray Mass Spectrometry

Since the discovery of the first linear chlorophyll catabolite, a PleB, 29 years ago in the leaves of barley,[1] the list of PleBs identified from different plant species has grown considerably; PleBs were shown to occur in a large structural variety arising from the conjugation of the tetrapyrrole core to hydrophilic residues.

With the first PxB (2), detected in leaves of katsura,[3] the spectrum of chlorophyll catabolites was extended beyond PleBs. Following the PxB (2) from katsura, investigations on other plant species have yielded PxBs; PxBs have been identified in leaf extracts of *Egeria densa*,[13] *Tilia cordata*,[14] plum tree,[15] and wych elm.[16] The abundances of PxBs compared to their PleB precursors, however, appeared to be lower. Exceptions to this observation are the PxBs discovered in the medicinal plant *Echinacea purpurea*, in which PxBs were detected in unprecedented abundance and diversity.[7] These findings raised the question of a broader occurrence of PxBs; since many plant species have been investigated before the discovery of PxBs, only PleBs are reported for those. The most common 3^2-OH PleB has been identified, among others, in *Cercidiphyllum japonicum*, spinach *(Spinacia oleracea)*, and *Spathiphyllum wallisii*.[17] Taken into account that PxBs hold a large promise of yet unexplored bioactivities, we re-investigated *Spinacia oleracea* and *Spathiphyllum wallisii*, reportedly containing 3^2-OH-PleB (1

EurJOC
European Journal of Organic Chemistry

Full Paper
doi.org/10.1002/ejoc.202000692

Chemistry
Europe
European Chemical
Societies Publishing

and **3**, respectively), but specifically looking for the presence of the 3^2-OH PxB (**2**).

A characteristic feature of PleBs, which originally led to the term "rusty pigments", is that when applied to thin-layer chromatography on silica gel, the colorless PleB spots developed first into yellow spots, and eventually into rust-colored spots under exposure to daylight.[3] Since the oxidation of PleBs to PxBs is influenced by air and light, higher apparent abundances of PxBs might be artifacts of the extraction procedure. We, therefore, used a combination of paper spray and leaf spray mass spectrometry which allowed the rapid and direct analysis of the leaf tissue without any sample preparation. Paper spray as well as leaf spray are rather new applications in the field of ambient mass spectrometry, which were first described by Liu et al. in 2010[18] and 2011.[19] In general, mass spectrometry has been developed into an efficient tool for identification and structural elucidation of phyllobilins with known modification patterns. The core structure of the linear tetrapyrroles has been characterized extensively for more than 20 different examples leading to the creation of an MS database for phyllobilins.[20] Due to characteristic fragmentation patterns of phyllobilins, MS and MS/MS are straightforward tools for the characterization of this family of linear tetrapyrroles.[21]

Paper spray MS analysis of freshly collected, senescent leaves (Figure 2 and Figure 3) clearly revealed the presence of both types of chlorophyll catabolites, colorless PleB and yellow PxB, in the intact senescent leaves of *Cercidiphyllum japonicum* as well as *Platanus occidentalis, Spinacia oleracea,* and *Spathiphyllum wallisii*. PleBs and PxBs were identified with respect to the fragmentation behavior of their isolated molecular ions in the gas phase.[21] Collision induced dissociation (CID) of the monoisotopic, potassiated molecular ions ([M + K]$^+$) of 3^2-OH PleB (**1** and **3**) at $m/z = 683$ showed diagnostic fragments at $m/z = 651$, which correspond to the characteristic loss of methanol (–32 Da). Interestingly, the two most abundant fragment ions of monoisotopic, potassiated molecular ions ([M + K]$^+$) of 3^2-OH PxB (**2**) at $m/z = 681$ correspond to the loss of methanol (–32 Da) as well as to the loss of water (–18 Da). The paper spray confirms the occurrence of PxB (**2**) in all four investigated plant species, for which only the PleB precursor (**1** or **3**) was reported before.
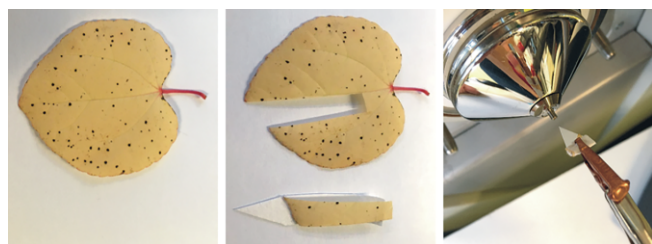

Figure 2. Example of a paper spray setup. The yellow, freshly collected senescent leaf from katsura tree (*Cercidiphyllum japonicum*, left) was cut using razor blade (center). The 0.5 cm × 3 cm slice was wrapped using a tapered piece of filter paper and mounted in front of the MS inlet (right). A potential of 3.5 kV was applied to the wrapped leaf, and the MS^n data were recorded within 30 s while applying 20 µL of methanol.
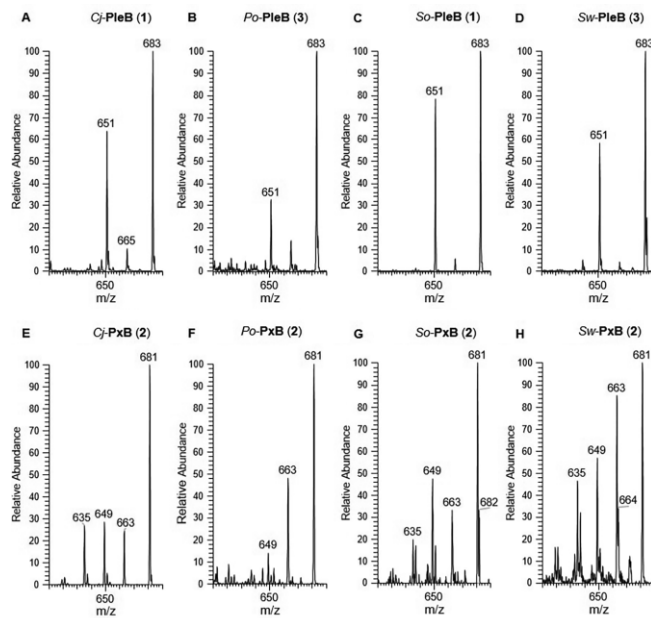

Figure 3. Direct mass spectrometric identification of PleB (**1** or **3**), and PxB (**2**) in senescent leaves of *Cercidiphyllum japonicum* (A, E), *Platanus occidentalis* (B, F), *Spinacia oleracea* (C, G) and *Spathiphyllum wallisii* (D, H) using paper spray analysis. (A–D): the monoisotopic, potassiated molecular ions ([**1,3** +K]$^+$) at m/z 683 were isolated and fragmented using CID. The loss of methanol (–32 Da) was found to be the most abundant fragmentation. (E-H): CID fragmentation pattern of the monoisotopic, potassiated molecular ions ([M + K]$^+$) of PxB (**2**) at m/z 681. The most prominent fragmentations were found to be the loss of water (–18 Da) as well as the loss of methanol (–32 Da).

Cytotoxic Potential of Phyllobilins

Structurally, phyllobilins bear a remarkable resemblance to heme-derived bilins;[22] whereby PxB, at least structurally, appears to be the bilirubin plant counterpart.[8] The bilins as well as the phyllobilins were long thought to be mere waste products, generated in a detoxification process of heme;[23] this assumption still holds true for the products of the chlorophyll degradation pathway. For the bilins, this paradigm has been disproved; e.g. bilirubin was shown to act as an important physiological antioxidant and to possess cytoprotective potential against various diseases.[24] In addition, dependent on the concentration as well as the state of redox homeostasis in the cell, bilirubin can also act as a cytotoxic agent.[25] This cytotoxicity plays a role in the anti-cancer effects attributed to the heme catabolite, among which anti-tumoral effects on human adenocarcinoma,[26] and apoptosis-inducing activity in colon cancer cells were described.[9]

The growing evidence for physiological activities of the bile pigments fueled the search for relevant properties of phyllobilins. In a first report, Müller et al. were able to demonstrate in vitro antioxidative activities for PleBs isolated from the peels of apples and pears.[27] For the PxBs, we recently reported their potent antioxidative activity in vitro; in addition, PxBs turned out to be rapidly taken up by cells, to be potent ROS scavengers in cells and to possess the ability to protect cells from oxidative stress.[7]

Further bio-relevant effects on cells, however, still remain to be elucidated. In this study, we set out to probe the cytotoxic

EurJOC
European Journal of Organic Chemistry

Full Paper
doi.org/10.1002/ejoc.202000692

Chemistry Europe
European Chemical
Societies Publishing

potential of phyllobilins on cancer cells; in a first experiment, we tested the PleB from katsura tree *Cj*-PleB (**1**) and its epimer from plane tree leaves *Po*-PleB (**3**) on two different human cancer cell lines, the highly invasive epithelial breast cancer MDA-MB-231 cell line and the urinary bladder carcinoma T24 cell line. **1** and **3** showed no significant inhibition of cell proliferation over 72 h in the tested concentration range of 1 to 100 μM (Figure 4A).
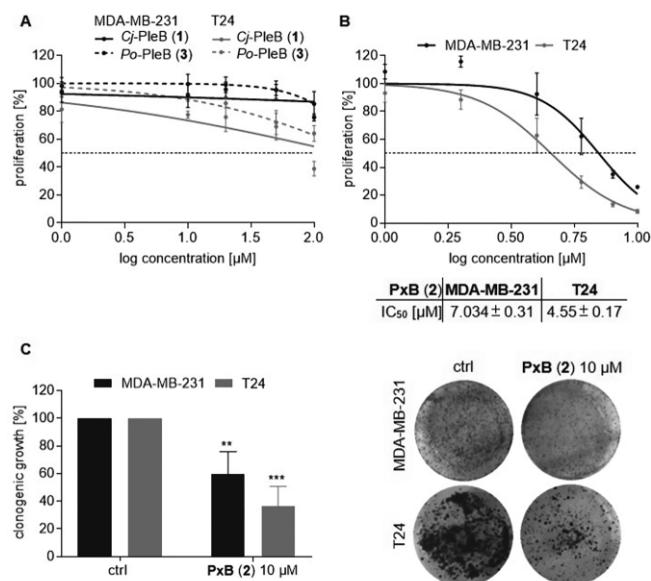

Figure 4. Effect of *Cj*-PleB (**1**) and *Po*-PleB (**3**), and PxB (**2**) on proliferation of T24 and MDA-MB-231 cancer cells. A) Treatment of T24 and MDA-MB-231 cells with **1** and **3** showed no anti-proliferative effect. B) **2** inhibits proliferation of T24 and MDA-MB-231 cells. Cells were treated with compound for 72 h and cell proliferation was assessed by crystal violet staining. C) **2** inhibits colony formation of T24 and MDA-MB-231 cells. PxB (**2**) treated cells were re-seeded and colony formation was assessed by crystal violet assay after one week.

For testing the cytotoxic potential of PxB (**2**), *Cercidiphyllum japonicum* was used as a source for the isolation of **1** and its subsequent oxidation; hence, only *Cj*-PxB (**2**) was used as test reagent and further defined as PxB (**2**), since *Cj*-PxB (**2**) and *Po*-PxB (**2**) are identical compounds due to the unsaturation of the stereocenter at C16 of the PleB (**1** or **3**). In contrast to the PleB precursors (**1** or **3**), **2** exhibited a potent anti-proliferative effect at low micromolar doses in both cell lines with calculated IC$_{50}$ values of 7.0 μM against MDA-MB-231 cells and 4.6 μM against T24 cells (Figure 4B).

Phylloxanthobilin Inhibits Colony Formation

Having established that **2** inhibits the proliferation of two different cancer cell lines, we further investigated this effect by a colony formation assay. This assay assesses the ability of single cells to grow and form colonies after a short time exposure to the compound by a crystal violet staining. The results showed a steep decline of colony formation in comparison to the DMSO vehicle control after brief exposure to 10 μM **2**, indicating **2** to inhibit also long-term survival and proliferation of cancer cells (Figure 4C).

Phylloxanthobilin Induces Apoptosis and a G2/M Cell Cycle Arrest

Furthermore, we assessed the cytotoxic potential of PxB (**2**) by flow cytometry, using a commercial Annexin V/PI staining kit, which allows for the distinction between different types of cell death. FITC conjugated Annexin V targets apoptotic cells and counterstaining with PI identifies cells undergoing early apoptosis (A+/PI-) or late apoptosis (A+/PI+). In contrast, cells with PI positive and Annexin V negative signal are related to a non-apoptotic, necrotic cell death.

The experiment showed that PxB (**2**) induced cell death in a dose-dependent manner with up to overall 30 % dead cells after 24 h, increasing to 45 % after 48 h in T24 cells (Figure 5, A and B). Early and late apoptotic cells, characterized by the

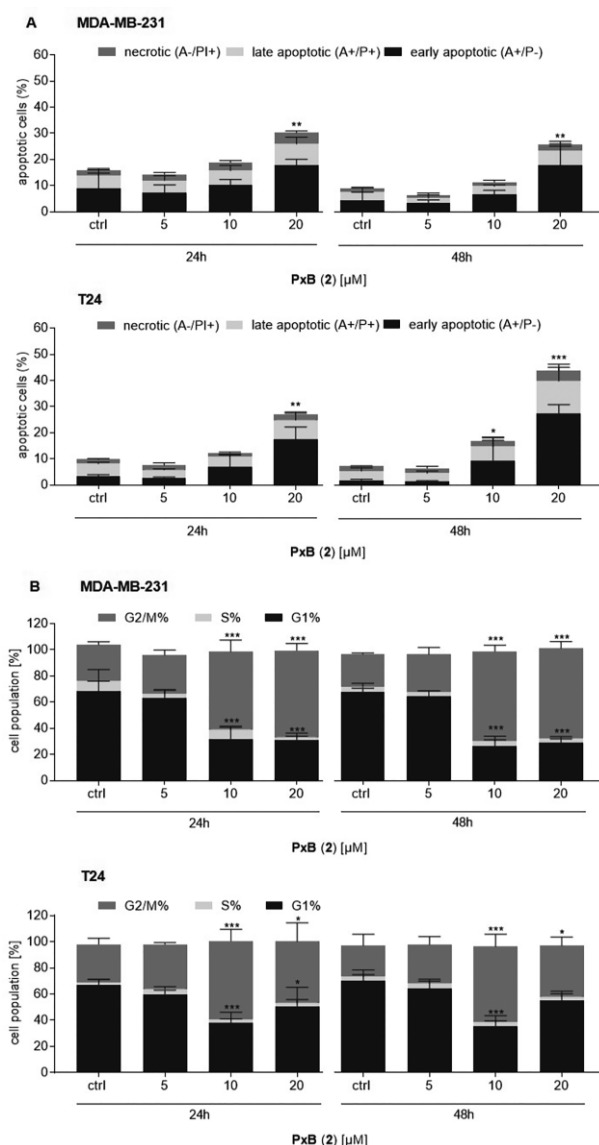Figure 5. PxB (**2**) induces apoptosis and a G2/M cell cycle arrest in MDA-MB-231 and T24 cells. A) Cells were incubated with **2** for 24 and 48 h, and cell death was analyzed by flow cytometry using Annexin V/PI co-staining. B) Cell cycle distribution of **2** treated MDA-MB-231 and T24 cells was assessed by PI staining and analyzed by flow cytometry, revealing that **2** causes a cell cycle arrest in the G2/M phase.

EurJOC
European Journal of Organic Chemistry

Full Paper
doi.org/10.1002/ejoc.202000692

Chemistry
Europe
European Chemical
Societies Publishing

Annexin V positive/PI negative (A+/PI-) and Annexin V positive/ PI positive (A+/PI+) signal, were increased upon PxB treatment. For necrotic cells, characterized by (A-/PI+), only a slight increase was observed. Taken together, these results demonstrate that **2** is a potent inducer of apoptotic cell death.

We further analyzed the cell death-inducing properties of PxB (**2**) on the cell cycle progression of T24 and MDA-MB-231 cells by PI staining according to the protocol of Nicoletti et al.[28] This method estimates the cellular DNA content by flow cytometry, allows for the quantitative analysis of cells in subG1, G1, S, and G2/M cell cycle phase, and detects cell cycle perturbations (Figure S6). Treatment with 10 µM and 20 µM **2** for 24 h or 48 h resulted in an arrest of cells in the G2/M cell cycle phase (Figure 5, C and D). The proportion of cells in G1 phase decreased significantly, in parallel with an increase of cells in the G2/M phase. In contrast, no effect on the population in the S phase was observed during treatment with **2**. Moreover, a significant increase of cells in the subG1 phase in both cell lines was observed, confirming the results of the Annexin V/PI assay that **2** promotes apoptotic cell death (Figure S7).

Cytotoxicity of PleB Can Be Tuned by Esterification

So far, PleBs have been identified and characterized as approximately 20 different structures, whereby identical PleBs have been isolated from different plant species. All PleBs share the same core structure with four deconjugated pyrrole units. Differences arise from modifications of the rings at four different positions (with the exception of a catabolite from *Arabidopsis thaliana*, which is speculated to result from an incomplete reduction from Chl b to Chl a[29]).

Of particular interest is the esterification of the propionic acid side chain at C12; Oberhuber et al. showed that introducing a methyl ester at the PluB stage by chemical synthesis changed the kinetics of the conversion to PleBs, resulting in increased stability of the esterified PluB.[12b] An esterification of the propionic acid side chain of PBs was also discovered to occur naturally, causing PluBs in banana peels to accumulate and, as a consequence, the peel of ripened bananas to luminesce blue.[30] On the PleB level, esterified compounds were identified in leaves of *Vitis vinifera*[31] and wych elm,[16] and very recently on the PxB level in *Epipremnum aureum*.[32]

In comparison to the PxB, the PleBs as more polar molecules showed no effect on the proliferation of cancer cells. We therefore modified the structure of the PleB by esterification of the propionic acid side chain aiming to decrease its polarity. For our experiments, we used *Cj*-PleB (**1**) as representative compound. We prepared four different esters of the propionic acid side chain with increasing length of the alkyl side chain as described in the experimental section to gradually decrease polarity (Figure 6). Chemical structures were confirmed by HRMS, ESI MS/MS and NMR measurements (Figure S8–S12, Table S3,4).

Indeed, the inhibitory effects on the proliferation of MDA-MB-231 and T24 cells were influenced by esterification, with activities increasing with the chain lengths of the alkyl esters (Figure 7). In MDA-MB-231 cells, the IC_{50} value of the methyl- compared to the ethyl ester showed a decrease with polarity (46.1 µM for the methyl ester (**4**) and 30.9 µM for the ethyl ester (**5**)), and even lower values were observed for the butyl ester (**6**), as well as for the octyl ester (**7**); butyl ester (**6**) exhibited a IC_{50} value of 23.6 µM and octyl ester (**7**) of 16.3 µM. The results for T24 cells showed similar IC_{50} values for **4** and **5** of around 17 µM; the IC_{50} was lower for the **6** (11.0 µM) and as low as 3.4 µM for **7**.

Thus, we reasoned that polarity might be a factor that plays a role in the observed differences in cytotoxic potential between PleBs.

Uptake of PxB (2), PleBs (1, 3), and Esterified PleBs (4–7) by Cancer Cells

A crucial factor for the efficacy of a therapeutic agent is the delivery into the cell, as most of the substances target intracellular constituents. The ability for small drugs to overcome the natural barrier of the cell, the plasma membrane, is mainly determined by the size and lipophilicity of the compound. Whereas lipophilic small molecules can easily enter the cell e.g. through diffusion or active transport, a weak membrane permeability limits the cellular uptake of hydrophilic or larger molecules. Therefore, a common method to improve bioavailability is to alter the lipophilicity of molecules by generating prodrugs.[33]

Although the mechanism of the cellular uptake for phyllobilins remains to be elucidated, the polarity of the different
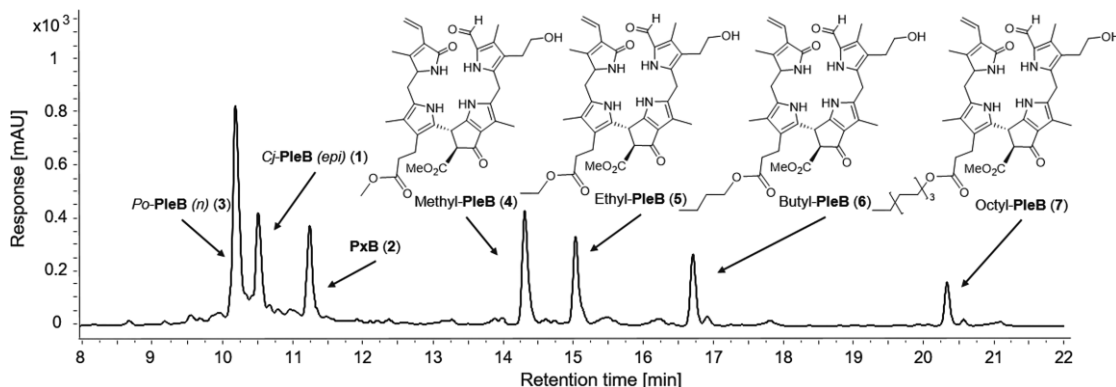

Figure 6. Analytical HPLC trace of a mixture of *Po*-PleB (**3**), *Cj*-PleB (**1**), PxB (**2**) and *Cj*-PleB-esters (**4–7**) (detection at 320 nm), showing a broad polarity range (linear gradient up to 17 min, see Experimental Section).
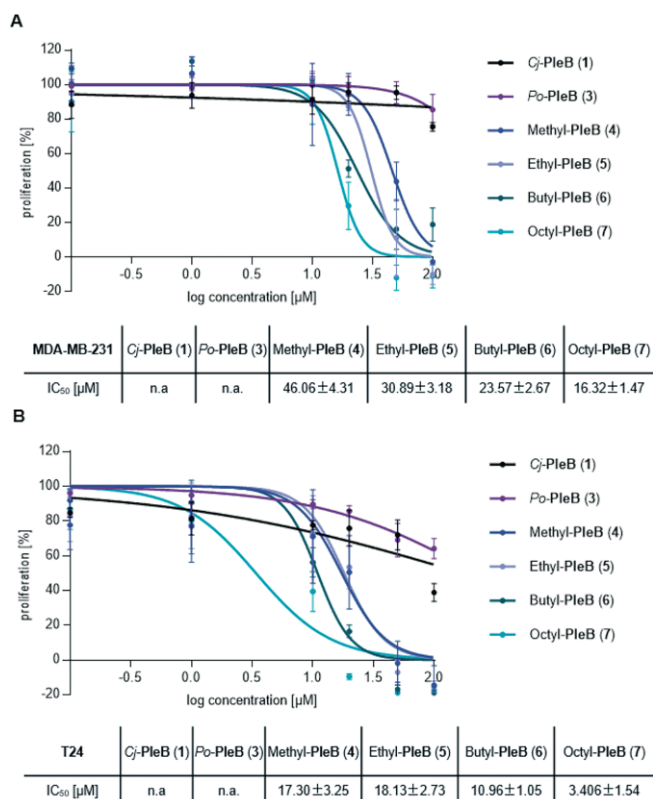
EurJOC
European Journal of Organic Chemistry

Full Paper
doi.org/10.1002/ejoc.202000692

Chemistry Europe
European Chemical
Societies Publishing

Figure 7. Esterification of *Cj*-PleB (**1**) influences the anti-proliferative activity. Cell proliferation assay of *Po*-PleB (**3**), *Cj*-PleB (**1**), PleB-esters (**4–7**) in MDA-MB-231 (A) and T24 (B) cells analyzed by crystal violet staining and corresponding IC_{50} values were calculated.

tetrapyrrolic compounds seems to be a factor influencing the cytotoxicity. We, therefore, investigated the uptake of different PBs by cells, using HPLC to quantify the PB signal from cell lysates. This experiment also aimed at clarifying whether the PleB-esters (**4–7**) act like prodrugs, serving as vehicles of the compounds into the cells. In this case, the esters are cleaved by cellular esterases afterward, leading to an increase of the effective concentration of PleB (**1**) in the cell compared to the use of the un-esterified compound; it could also be the case, however, that the esterified PleB itself has a cytotoxic activity.

All tested compounds could be found in the lysates of T24 cells, confirming that PBs, in general, can be taken up by cancer cells and are stable under the indicated conditions (Figure S13). In comparison to the PxB (**2**), the *Cj*-PleB (**1**) and *Po*-PleB (**3**) were only detected in minute amounts (Figure 8). This indicates the lack of cytotoxicity of the PleB (**1,3**) to correlate with higher polarity and lower intracellular compound concentration.

In contrast, the esterified PleBs (**4–7**) were detected in high concentrations. As expected, the intracellular concentration increased in parallel with apolarity of the compounds, being lowest for the methylated PleB (**4**) and highest for the butylated PleB (**6**). For the most apolar octylated PleB (**7**), however, a decreased intracellular concentration was observed, which might be due to low solubility in medium (Figure 8).

Interestingly, only minute amounts of hydrolyzed "free" PleB (**1**) could be observed in cell lysates when treating cells with the PleB-esters (**4–7**) (Figure S8). These results indicate the anti-
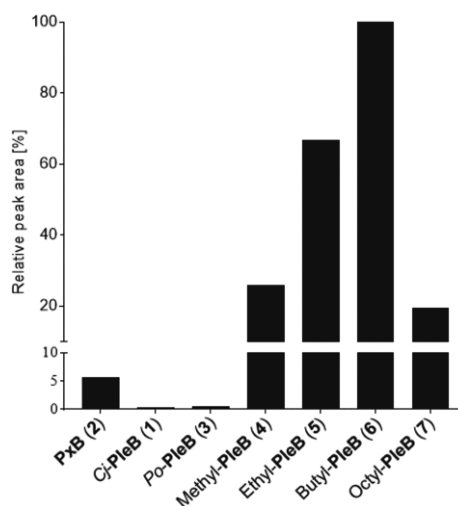

Figure 8. Esterification leads to higher amounts of intracellular compound. Cellular uptake of PxB (**2**), *Cj*-PleB (**1**), and *Po*-PleB (**3**) and *Cj*-PleB-esters (**4–7**) in T24 cells. A discontinuous y axis is shown for better visibility of the (low) uptake of **1** and **3**. Cells were treated with compounds (80 μM) for 5 h, lysed by beat beating, and the supernatant was analyzed by analytical HPLC.

proliferative effects of **4–7** not to depend on the liberation of the "free" PleB (**1**) in the cell. More likely, the esters appear to exhibit cytotoxic activities themselves, which cannot be explained by a prodrug mechanism. The observed reactivity of the PxB (**2**), however, surpasses the activity of **4** and **5**. Although the IC_{50} values of **6**, **7**, and **2** in T24 cells are in a similar low micromolar range, **6** and **7** showed a significantly lower polarity than the PxB **2** (Figure 6) and a higher uptake (Figure 8). Nevertheless, neither polarity nor uptake can account for the difference in potency between PleBs and PxB (**2**). This indicates the structural difference between PleB and PxB, manifested by a double bond, to play a crucial role in inhibiting proliferation of cancer cells.

Whether a PleB-ester acts as a prodrug and the ester gets cleaved by cellular esterases, or the esterified compound itself is the cytotoxic agent, needs yet to be resolved in more detail; our results indicate, however, that only minute amounts of hydrolyzed PleB (**1**) are present in the cells, even 5 h after treatment.

Conclusion

In this study, we identified plane tree as novel source for 3^2-OH-PxB (**2**). This yellow chlorophyll catabolite was shown to be more abundant in Nature than previously thought, as was shown by paper spray MS; we demonstrated the occurrence of PxB (**2**) in leaves of *Spinacia oleracea* and *Spathiphyllum wallisii*, for which only the common 3^2-OH PleB (**1** or **3**) has been reported previously. After all, the discovery of PleBs precedes the discovery of PxBs by 17 years, therefore the studies during that time range did not screen for PxBs. Whether PxBs fulfill biological roles for plants, has yet to be investigated.

Here, we could introduce PxB (**2**) as potent anti-cancer agent in human cells, inhibiting proliferation in the low micromolar range, inducing apoptosis, and causing a G2/M cell cycle arrest.

EurJOC
European Journal of Organic Chemistry

Full Paper
doi.org/10.1002/ejoc.202000692

Chemistry Europe
European Chemical
Societies Publishing

We provide first evidence for anti-cancer activities of PxBs and add another proof that chlorophyll catabolites are more than mere waste products of a degradation pathway.

The discovery of a potent activity for the PxB (**2**), the fact that the cytotoxicity of PleBs (**1,3**) on cancer cells is tunable by a simple modification of the compounds, and the abundance of this family of natural products in the plant kingdom, open the door for further investigations of the anti-tumoral potential of the phyllobilins. Future studies will deal with the mechanism behind the potent killing and apoptosis induction in cancer cells and aim at identifying new sources of PxBs, which hold a large promise to reveal yet to be explored bioactivities.

Experimental Section

General: HPLC grade acetonitrile (ACN), methanol (MeOH), ethanol (EtOH), butanol, octanol, dimethyl sulfoxide (DMSO), hydrochloric acid (HCl), dichloromethane (DCM) and silica gel 60 were obtained from VWR International GmbH (Ismaning, Germany) and ultra-pure water (18 MΩ cm^{-1}) from a Millipore S.A.S. Milli-Q Academic system (18.2 MΩ cm-1, Molsheim, France). Potassium phosphate dibasic (K_2HPO_4), Potassium phosphate monobasic (KH_2PO_4), ammonium acetate (NH$_4$AcO), glass beads (acid washed, 425–600 μm), (benzotriazol-1-yloxy)tripyrrolidinophosphonium hexafluorophosphate (PyBoP), Triethylamine (Et$_3$N), and [D$_4$]methanol were from Sigma-Aldrich (Taufkirchen, Germany) and SepPak Plus C18 cartridges from Waters Associates (Milford, USA). DMEM medium, penicillin, and streptomycin were from PAN-Biotech (Aidenbach, Germany); fetal calf serum (FCS) was from PAA Laboratories GmbH (Pasching, Austria) and Triton X-100 was from Merck (Darmstadt, Germany). Crystal violet, propidium iodide (PI) and trisodium citrate were purchased from Carl Roth (Karlsruhe, Germany) and sea sand from Fisher Scientific (Waltham, MA, USA).

Human bladder cancer cell line T24 and highly invasive human triple negative breast adenocarcinoma cell line MDA-MB-231 were obtained from the *Deutsche Sammlung von Mikroorgansimen und Zellkulturen* (DSMZ; Braunschweig, Germany) and maintained in DMEM medium supplemented with 10 % fetal calf serum (FCS) and 1 % penicillin/streptomycin. Cells were cultured at 37 °C under 5 % CO$_2$ atmosphere with constant humidity in 75 cm^3 tissue culture flasks.

Plant Material: Katsura trees (*Cercidiphyllum japonicum*) were located outside of the botanical garden Munich using the tree-finder app https://www.botmuctrees.de/. Senescent leaves were collected in the Maria-Ward-Straße, Munich (48°09′41.0″N 11°29′58.8″E). Senescent leaves of plane tree (*Platanus occidentalis*) were collected from trees in the Feodor-Lynen Straße at the campus Großhadern of the University of Munich (48°06′48.6″N 11°27′56.2″E). Spinach was obtained from a local supermarket and stored in the dark for 3 days to induce Chl breakdown. *Spathiphyllum wallisii* was bought at a local garden center. A senescent leaf was collected directly from the plant.

The identity of the plant material was determined by Prof. Susanne S. Renner (Department of Systematic Botany and Mycology, Faculty of Biology, University of Munich); Voucher specimen of *Platanus occidentalis (*Moser & Karg 2)*, Cercidiphyllum japonicum (*Moser & Karg 3)*, and *Spathiphyllum wallisii (*Moser & Karg 4) have been deposited in the Munich herbarium (acronym M).

Chromatography: i) Analytical HPLC: Agilent 1260 Infinity II LC system with a 1260 Infinity Degasser, a 1260 Series quaternary pump

and 1260 Series diode array detector; Merck LiChrospher® 60 RP-select B (5 μm) LiChroCART® 125–4, protected by a Merck LiChrospher® 100 RP̄18 (5 μm) LiChroCART® 4–4 i.d. pre-column; injection volume: 100 μL (unless stated otherwise). Solvent system: mobile phase A = NH$_4$AcO buffer 10 mM pH 7, B = ACN, flow 0.5 mL/min; Solvent composition: 0–2 min 5 % B, 2–17 min 5 % to 70 % B, 17–20 min 70 % to 100 % B, 20–22 min 100 % B, 22–24 min 100 to 5 % B. Data were processed with OpenLab CDS Data Analysis 2.3.

ii) Semi-preparative HPLC: Gynkotek LC-System with manual sampler, M480 pump, Phenomenex DG-301 online degasser, Gynkotek UVD 640 diode array detector and a Rheodyne injection valve with 5 mL loop; column: Supelco Ascentis® C18, 5 μm, 15 cm × 10 mm, with a Phenomenex pre-column ODS 9 × 16 mm; mobile phase A = NH$_4$AcO buffer 10 mM pH 7, B = MeCN, flow 2.5 mL/min; solvent composition: 0–2 min 12 % B, 2–12 min 12 % to 20 % B, 12–30 min 20 % to 80 % B, 30–40 min 80 % to 100 % B. Data were processed with Gynkosoft 5.50.

Spectroscopy: UV/Vis: Thermo Spectronic Genesys 5 (336001) UV Visible spectrophotometer; λ_{max} in nm (rel. ε). Concentrations of PleB and PleB-esters were calculated using log ε (312 nm) = 4.23,[4] concentrations of PxB were calculated using log ε (426 nm) = 4.51.[3]

Paper spray mass spectrometry: Thermo Scientific Orbitrap XL mass spectrometer. The freshly collected senescent (yellow) leaves were cut into 0.5 cm × 3 cm slices using a razor blade. A freshly cut slice was wrapped into a tapered piece of filter paper and mounted in front of the MS inlet at a distance of 0.5 cm. A high voltage potential of 3.5 kV was applied to the wrapped leaf and MS^n data were recorded within 30 s while 20 μL of methanol were dropped onto the filter paper.

HRMS were measured at the MS facility of the Department of Chemistry, University of Munich. Data were processed with Xcalibur.

NMR spectra were recorded on an Avance III HD 500 MHz NMR spectrometer from Bruker BioSpin equipped with a CryoProbe™ Prodigy broadband probe using CD$_3$OD as solvent. Assignments of ^{13}C signals determined from ^{1}H,^{13}C heteronuclear correlations in HMQC and HMBC spectra. NMR data were analyzed with Mestre Nova 14.1.1.

During all handling steps, the material was protected from light and temperatures above 37 °C were avoided unless stated otherwise.

HPLC Analysis of Plane Tree (*Platanus occidentalis*) PBs: 16 cm^2 of a senescent leaf of plane tree was mixed with sea sand and 2 mL of MeOH in a mortar. The slurry was centrifuged (1000 rpm, 5 min, 4 °C), and a 40 μL aliquot of the supernatant was diluted with 160 μL of phosphate buffer (pH 7.4); a 100 μL aliquot was applied to analytical HPLC. In a co-elution experiment, isolated pure samples *Po*-PleB (**3**) and *Po*-PxB (**2**), respectively, were applied to analytical HPLC. *Cj*-PleB (**1**) and *Cj*-PxB (**2**) were isolated from katsura leaves as described below and were analyzed the same way. In addition, a 1:1 mixture of **1** and **3**, and of **2** from the two different plant sources, respectively, were analyzed by HPLC.

Large Scale Isolation of PleB from Senescent Leaves of Katsura (*Cercidiphyllum japonicum*) and Plane Tree (*Platanus occidentalis*): Senescent leaves of katsura and plane tree were extracted as follows (optimized protocol for plane tree described): 300 g of frozen leaves were ground in a 5 L stainless steel beaker using a Braun hand blender Model MR 5000 and extracted with hot water (1200 mL). The mixture was filtered through a cotton cloth and the residue was again washed with hot water (500 mL). The mixture was cooled to room temperature before extracting twice with 200 mL of DCM. The DCM solution was applied to a silica column (50 mm

EurJOC
European Journal of Organic Chemistry

Full Paper
doi.org/10.1002/ejoc.202000692

Chemistry Europe
European Chemical
Societies Publishing

diameter, 300 mm length, 70 g silica gel 60). The column was washed with DCM, and PBs were eluted with increasing MeOH (DCM/MeOH, 95:5, 80:20, 50:50). The different fractions were analyzed by TLC, PB containing fractions were combined, and the solvent was evaporated. The obtained residue was dissolved in MeOH/ potassium phosphate buffer (pH 7.4) and purified by semi-preparative HPLC. Yields were 50 mg (77.6 μmol) of **3** and 10 mg (15. 6 μmol) of **2**.

Solid-Phase Synthesis of PxB (2) by Oxidation of *Cj*-PleB (1) and *Po*-PleB (3): 10 mg PleB (**1** or **3**) were dissolved in 5 mL of DCM and 1 mL of MeOH and added to 7 g of silica. The mixture was carefully dried under vacuum and the powder was stirred overnight under a tungsten light bulb. The complete formation of **2** was confirmed by analytical HPLC, the reaction mixture was eluted with EtOH, filtered through a paper filter and the solvent was evaporated on a rotary evaporator. The crude product was purified by semi-preparative HPLC. Fractions containing **2** were pooled and dried by means of a rotary evaporator. The residue was dissolved in ACN/ potassium phosphate buffer (pH 2.5) 20:80 and stirred overnight. After SPE (Sep-Pak-C18 cartridge 5 g), pure **2** was eluted with ACN and dried under vacuum. 2 mg (3.1 μmol, 20 %) of **2** were obtained. DMSO stocks were prepared and stored at –20 °C until further use.

Esterification of *Cj*-PleB (1): For synthesis of methyl-PleB (**4**), 4 mg **1** were dissolved in 1 mL of DMSO and 10 μL of MeOH, 2.5 μL of Et$_3$N, and 4.5 mg of PyBoP were added. The mixture was stirred at room temperature overnight. The formation of **4** was confirmed by analytical HPLC. The mixture was purified by semi-preparative HPLC, yielding 1.6 mg (2.4 μmol, 40 %) of **4**.

Syntheses of **5–7** were performed according to the protocol of Li and Kräutler with minor modifications.[5] PyBoP and Et$_3$N were used instead of BOP and TEA. **1** was dissolved in either ethanol, butanol or octanol, followed by addition of the coupling reagents. The formation of the PleB-esters (**5–7**) was confirmed by analytical HPLC. 58 % (1.1 μmol) of ethyl-PleB (**5**), 61 % (1.2 μmol) of butyl-PleB (**6**), and 65 % (1.4 μmol) of octyl-PleB (**7**) were obtained.

Spectroscopic Data: Retention time (t_R) from analytical HPLC.

***Cj*-PleB (1):** t_R = 10.5 min. UV/Vis online spectrum (nm, rel ε): 220 (1.00), 242 (0.8), 314 (0.72) nm. HRMS (ESI): $m/z_{calculated}$ (C$_{35}$H$_{41}$O$_8$N$_4$) = 645.29189 [M + H]$^+$; m/z_{found} = 645.29216 (Δ = 0.4 ppm).

***Cj*-PxB (2):** t_R = 11.3 min. UV/Vis online spectrum (nm, rel ε): 212 (0.94), 246 (0.51), 314 (0.66), 426 (1.00) nm. HRMS (ESI): $m/z_{calculated}$ (C$_{35}$H$_{39}$O$_8$N$_4$) = 643.27624 [M + H]$^+$; m/z_{found} = 643.27679 (Δ = 0.9 ppm).

***Po*-PleB (3):** t_R = 10.2 min. UV/Vis spectrum (λ_{max}/nm, log ε): 220 (4.66), 245 (4.28), 310 (4.23) nm (see Figure S1). HRMS (ESI): $m/z_{calculated}$ (C$_{35}$H$_{41}$O$_8$N$_4$) = 645.29189 [M + H]$^+$; m/z_{found} = 645.29245 (Δ = 0.9 ppm).

^{1}H NMR (500 MHz, CD$_3$OD): δ [ppm] = 1.89 (s, H$_3$C17^1), 1.94 (s, H$_3$C13^1), 2.10 (s, H$_3$C7^1), 2.26 (s, H$_3$C2^1), 2.32 (m, H$_2$C12^2), 2.50 (dd, J = 14.5/8.9, H$_A$C15), 2.63 (m, H$_2$C12^1), 2.73 (m, H$_2$C3^1), 2.82 (dd, J = 14.3/5.2, H$_B$C15), 3.47 (m, H$_2$C3^2), 3.74 (s, H$_3$C8^4), 3.85 (m, HC8^2), 3.94 (m, H$_2$C5), 4.06 (m, HC16), 4.91 (s, HC10), 5.31–5.37 (m, H$_A$C18^2), 6.09 (dd, J = 17.7/2.4, H$_B$C18^2), 6.44 (dd, J = 11.7/17.8, HC18^1), 9.36 (s, HC20) (Table S1). ^{13}C NMR (500 MHz, CD$_3$OD): δ [ppm] = 8.06 (2^1), 8.06 (13^1), 8.06 (7^1), 11.92 (17^1), 20.93 (12^1), 20.93 (3^1), 22.65 (5), 27.36 (15), 35.94 (10), 38.52 (12^2), 50.96 (8^4), 59.54 (16), 61.26 (3^2), 111.06 (7), 114.2 (13), 119.59 (3), 117.03 (18^2), 119.59 (12), 123.18 (11), 124.52 (8), 126.04 (18^1), 127.22 (18), 128.11 (1), 133.05 (6), 133.95 (2), 137.09 (4), 155.94 (17), 160.43 (9), 170.31 (8^3), 173.0 (19), 176.23 (20), 180.18 (12^3), 192.75 (8^1) (Table S1).

***Po*-PxB (2):** t_R = 11.3 min. UV/Vis spectrum (λ_{max}/nm, log ε): 228 (4.99), 248 (4.51), 310 (4.61), 429 (4.51) nm (see Figure S1). HRMS (ESI): $m/z_{calculated}$ (C$_{35}$H$_{39}$O$_8$N$_4$) = 643.27624 [M + H]$^+$; m/z_{found} = 643.27652 (Δ = 0.4 ppm).

^{1}H NMR (500 MHz, CD$_3$OD): δ [ppm] = 1.98 (s, H$_3$C7^1), 2.12 (s, H$_3$C13^1), 2.16 (s, H$_3$C17^1), 2.19 (s, H$_3$C2^1), 2.37 (m, H$_2$C12^2), 2.64 (m, H$_2$C3^1), 2.70 (m, H$_A$C12^1), 2.79 (m, H$_B$C12^1), 3.59 (m, H$_2$C3^2), 3.78 (s, H$_3$C8^4), 3.85 (m, HC8^2), 3.96 (m, H$_2$C5), 5.01 (HC10), 5.34 (m, H$_A$C18^2), 6.09 (d, J = 17.6, H$_B$C18^2), 6.19 (s, HC15), 6.49 (d, J = 15.0, HC18^1), 9.38 (s, HC20) (Table S2).

***Cj*-methyl-PleB (4):** t_R = 14.3 min. UV/Vis online spectrum (nm, rel ε): 216 (1.00), 242 (0.70), 312 (0.59) nm. HRMS (ESI): $m/z_{calculated}$ (C$_{36}$H$_{43}$O$_8$N$_4$) = 659.30754 [M + H]$^+$; m/z_{found} = 659.30724 (Δ = 0.5 ppm). MS/MS (ESI): m/z (%) = 659.1 (100, [M – H]$^+$); 627.0 (12, [M+H-CH$_4$O]$^+$); 474.2 (2, [M+H- CH$_4$O-ringA]$^+$).

^{1}H NMR (500 MHz, CD$_3$OD): δ [ppm] = 1.85 (s, H$_3$C13^1), 1.91 (s, H$_3$C17^1), 2.09 (s, H$_3$C7^1), 2.22 (s, H$_3$C2^1), 2.25 (m, H$_A$C12^2), 2.38 (m, H$_B$C12^2), 2.53 (m, H$_A$C15), 2.57 (m, H$_2$C3^1), 2.60 (m, H$_2$C12^1), 2.81 (dd, J = 14.6/5.5, H$_B$C15), 3.50 (m, H$_2$C3^2), 3.56 (m, H$_3$12^4), 3.71 (d, J = 3.2, HC8^2), 3.73 (s, H$_3$C8^4), 3.90 (d, J = 6.8, H$_2$C5), 3.99 (m, HC16), 4.82 (s, HC10), 5.31 (dd, J = 11.8/2.4, H$_A$C18^2), 6.05 (dd, J = 17.7/2.4, H$_B$C18^2), 6.40 (m, HC18^1), 9.31 (s, HC20) (Table S3). ^{13}C NMR (500 MHz, CD$_3$OD): δ [ppm] = 8.24 (2^1), 8.67 (7^1), 8.67 (13^1), 11.67 (17^1), 19.82 (12^1), 22.83 (5), 27.55 (3^1), 28.83 (15), 36.56 (10), 35.70 (12^2), 52.00 (8^4), 57.58 (12^4), 61.12 (16), 61.87 (3^2), 68.31 (8^2), 112.29 (7), 114.99 (13), 120.37 (3), 118.51 (18^2), 119.03 (12), 123.97 (14), 125.76 (8), 126.23 (18^1), 128.45 (18), 128.90 (1), 133.84 (6), 134.74 (2), 137.88 (4), 156.29 (17), 160.33 (9), 171.10 (8^3), 174.24 (19), 177.29 (20), 174.69 (12^3), 190.85 (8^1) (Table S3).

***Cj*-ethyl-PleB (5):** t_R = 15.1 min. UV/Vis online spectrum (nm, rel ε): 216 (1.00), 244 (0.71), 312 (0.58) nm. HRMS (ESI): $m/z_{calculated}$ (C$_{37}$H$_{45}$O$_8$N$_4$) = 673.32319 [M + H]$^+$; m/z_{found} = 673.32282 (Δ = 0.5 ppm). MS/MS (ESI): m/z (%) = 673.1 (100, [M + H]$^+$); 504.9 (16, [M+H-C$_2$H$_6$O-ringD]$^+$).

^{1}H NMR (500 MHz, CD$_3$OD): δ [ppm] = 1.14 (t, J = 7.0, H$_3$C12^5), 1.86 (s, H$_3$C13^1), 1.92 (s, H$_3$C17^1), 2.09 (s, H$_3$C7^1), 2.22 (s, H$_3$C2^1), 2.24 (m, H$_A$C12^2), 2.35 (m, H$_B$C12^2), 2.53 (m, H$_A$C15), 2.57 (m, H$_2$C3^1), 2.60 (m, H$_2$C12^1), 2.81 (dd, J = 14.6/5.4, H$_B$C15), 3.51 (m, H$_2$C3^2), 3.57 (q, J = 7.1, H$_2$12^4), 3.71 (d, J = 3.2 HC8^2), 3.73 (s, H$_3$C8^4), 3.90 (d, J = 6.3, H$_2$C5), 4.02 (m, HC16), 4.82 (s, HC10), 5.31 (dd, J = 11.7/2.4, H$_A$C18^2), 6.05 (dd, J = 17.7/2.4, H$_B$C18^2), 6.39 (dd, J = 17.8/11.7, HC18^1), 9.31 (s, HC20) (Table S3). ^{13}C NMR (500 MHz, CD$_3$OD): δ [ppm] = 8.24 (2^1), 8.24 (7^1), 8.67 (13^1), 11.67 (17^1), 17.68 (12^5), 19.82 (12^1), 22.83 (5), 27.12 (3^1), 29.26 (15), 36.56 (10), 36.13 (12^2), 52.00 (8^4), 57.58 (12^4), 60.67 (16), 61.87 (3^2), 68.31 (8^2), 111.84 (7), 114.54 (13), 119.93 (3), 118.50 (18^2), 118.58 (12), 123.52 (14), 125.31 (8), 125.80 (18^1), 128.01 (18), 128.45 (1), 133.39 (6), 134.29 (2), 137.43 (4), 155.84 (17), 159.43 (9), 170.65 (8^3), 173.79 (19), 174.24 (12^3), 177.28 (20), 190.85 (8^1) (Table S3).

***Cj*-butyl-PleB (6):** t_R = 16.7 min. UV/Vis online spectrum (nm, rel ε): 216 (1.00), 242 (0.71), 312 (0.57) nm. HRMS (ESI): $m/z_{calculated}$ (C$_{39}$H$_{49}$O$_8$N$_4$) = 701.35449 [M + H]$^+$; m/z_{found} = 701.35422 (Δ = 0.4 ppm). MS/MS (ESI): m/z (%) = 701.2 (100, [M + H]$^+$); 627.4 (8, [M+H-C$_4$H$_{10}$O]$^+$); 504.6 (21, [M+H-C$_4$H$_{10}$O-ringD]$^+$).

^{1}H NMR (500 MHz, CD$_3$OD): δ [ppm] = 0.87 (t, J = 7.4 H$_3$C12^7), 1.3 (m, H$_2$C12^6), 1.52 (m, H$_2$C12^5), 1.86 (s, H$_3$C13^1), 1.91 (s, H$_3$C17^1), 2.09 (s, H$_3$C7^1), 2.22 (s, H$_3$C2^1), 2.25 (m, H$_A$C12^2), 2.36 (m, H$_B$C12^2), 2.53 (m, H$_A$C15), 2.58 (m, H$_2$C3^1), 2.60 (m, H$_2$C12^1), 2.77 –2. 85 (m, H$_B$C15), 3.51 (m, H$_2$C3^2), 3.71 (d, J = 1.9 HC8^2), 3.73 (s, H$_3$C8^4), 3.90 (d, J = 6.1, H$_2$C5), 3.96 (m, HC16), 3.97 (m, H$_2$12^4), 4.82 (s, HC10), 5.31 (dd, J = 11.7/2.4, H$_A$C18^2), 6.05 (dd, J = 17.7/2.4, H$_B$C18^2), 6.39

EurJOC
European Journal of Organic Chemistry

Full Paper
doi.org/10.1002/ejoc.202000692

Chemistry Europe
European Chemical
Societies Publishing

(dd, J = 17.8/11.7, HC18[1]), 9.31 (s, HC20) (Table S4). ^{13}C NMR (500 MHz, CD$_3$OD): δ [ppm] = 8.24 (2[1]), 8.24 (7[1]), 8.67 (13[1]), 11.67 (17[1]), 12.35 (12[7]), 17.50 (12[6]), 19.82 (12[1]), 22.83 (5), 27.12 (3[1]), 29.26 (15), 30.37 (12[5]), 36.56 (10), 36.13 (12[2]), 52.00 (8[4]), 61.12 (16), 61.87 (3[2]), 63.84 (12[4]), 112.29 (7), 114.99 (13), 118.51 (18[2]), 119.03 (12), 120.37 (3), 123.97 (14), 125.76 (8), 126.23 (18[1]), 128.45 (18), 128.90 (1), 133.84 (6), 134.74 (2), 137.88 (4), 156.29 (17), 159.88 (9), 171.10 (8[3]), 174.24 (19), 174.69 (12[3]), 177.29 (20) (Table S4).

***Cj*-octyl-PleB (7):** t_R = 20.4 min. UV/Vis online spectrum (nm, rel ε): 216 (1.00), 242 (0.70), 310 (0.56) nm. MS/MS (ESI): $m/z_{calculated}$ (C$_{43}$H$_{57}$O$_8$N$_4$) = 757.41709 [M + H]$^+$; m/z_{found} = 757.41669 (Δ = 0.5 ppm). MS/MS (ESI): m/z (%) = 757.1 (100, [M + H]$^+$); 725.2 (6, [M+H-CH$_4$O]$^+$); 504.8 (18, [M+H-C$_8$H$_{18}$O-ringD]$^+$).

^{1}H NMR (500 MHz, CD$_3$OD): δ [ppm] = 0.85 (m, H$_3$C12[11]), 1.18–1.61 (m, H$_2$C12[7–10]), 1.46–1.61 (m, H$_2$C12[5], H$_2$C12[6]), 1.86 (s, H$_3$C13[1]), 1.91 (s, H$_3$C17[1]), 2.09 (s, H$_3$C7[1]), 2.22 (s, H$_3$C2[1]), 2.27 (m, H$_A$C12[2]), 2.33 (m, H$_B$C12[2]), 2.53 (m, H$_A$C15), 2.57 (m, H$_2$C3[1]), 2.60 (m, H$_2$C12[1]), 2.81 (dd, J = 14.6/5.4 H$_B$C15), 3.51 (m, H$_2$C3[2]), 3.71 (d, J = 3.3 HC8[2]), 3.73 (s, H$_3$C8[4]), 3.90 (d, J = 5.7, H$_2$C5), 3.97 (m, HC16), 3.97 (m, H$_2$12[4]), 4.82 (s, HC10), 5.31 (dd, J = 11.7/2.4, H$_A$C18[2]), 6.05 (dd, J = 17.8/2.4, H$_B$C18[2]), 6.39 (dd, J = 17.8/11.6, HC18[1]), 9.31 (s, HC20) (Table S4). [13]C NMR (500 MHz, CD$_3$OD): δ [ppm] = 8.24 (2[1]), 8.67 (7[1]), 8.67 (13[1]), 11.67 (17[1]), 13.82 (12[11]), 14.68 (12[10]), 20.25 (12[1]), 21.97 (12[9]), 22.83 (5), 25.40 (12[8]), 27.55 (3[1]), 28.83 (12[6]), 29.26 (15), 29.69 (12[7]), 31.84 (12[5]), 36.56 (10), 36.13 (12[2]), 52.00 (8[4]), 60.67 (16), 61.87 (3[2]), 64.87 (12[4]), 68.31 (8[2]), 111.85 (7), 114.54 (13), 118.51 (18[2]), 118.58 (12), 119.93 (3), 123.52 (14), 125.31 (8), 126.66 (18[1]), 128.01 (18), 128.45 (1), 133.39 (6), 134.29 (2), 137.43 (4), 155.84 (17), 159.43 (9), 170.65 (8[3]), 173.79 (19), 174.24 (12[3]), 177.29 (20) (Table S4).

Cell Proliferation Assay: Proliferation of PB treated T24 and MDA-MB-231 cells was determined by a crystal violet staining. 4×10^3 (MDA-MB-231) or 2.5×10^3 (T24) cells were seeded in 96 well plates and grown for 24 h. Cells were incubated with indicated concentrations of compounds for 72 h, followed by washing with PBS + and staining with 0.5 % crystal violet solution for 10 min. After washing the cells with water and drying overnight, crystal violet was redissolved with trisodium citrate solution, and absorption at 550 nm was measured with a SpectraFluor Plus plate reader (Tecan, Crailsheim, Germany). The number of viable cells was calculated by subtracting the average of the day 0 control values and normalizing to the corresponding DMSO control.

Clonogenic Assay: T24 and MDA-MB-231 cells were seeded at 3×10^5 cells/well in a 6 well plate and allowed to attach for one day, before incubating with PxB (**2**) (10 μM) and DMSO vehicle control for 24 h. Cells were harvested and re-seeded at 5000 cells/well for MDA-MB-231 and 3000 cells/well for T24 cells in 6 well plates in triplicates. After one week, cells were washed with PBS+, stained with 0.5 % crystal violet solution for 10 min and again washed with water. The plate was dried overnight and pictures of the colonies were captured with a digital camera (Canon DS126181). After the addition of trisodium citrate solution, the absorption was measured at 550 nm with a SpectraFluor Plus plate reader (Tecan, Crailsheim, Germany). The clonogenic growth of treated cells was normalized to the corresponding DMSO control.

Annexin V/PI Staining Assay: To quantify *Cj*-PxB (**2**) induced cell death, a co-staining with FITC conjugated AnnexinV (AnnV) and propidium iodide (PI) was performed with an AnnexinV/PI staining kit (Thermo Fisher Scientific, Waltham, MA, USA) according to the manufacturer's instructions. In brief, 3×10^4 cells were cultured in 24 well plates for 24 h before incubating with indicated concentrations of **2** for 24 or 48 h. Cells were harvested, washed with PBS,

and incubated with FITC conjugated AnnV in binding buffer for 10 min. After washing with binding buffer, PI solution was added and cells were immediately analyzed by a BD FACS Canto™ II cytometer. PI and AnnV negative cells were identified as living cells, PI negative and AnnV positive as early apoptotic cells, PI positive and AnnV positive as late apoptotic, and PI positive and AnnV negative as necrotic cells. Data were processed with FlowJo 7.6 software.

Cell Cycle Analysis Assay: The cell cycle distribution of T24 and MDA-MB-231 cells was determined by propidium iodide staining and flow cytometry according to the protocol of Nicoletti et al.[28] Briefly, 3×10^4 cells were seeded and allowed to attach for one day. Next, cells were treated with **2** (5, 10, 20 μM), and DMSO as a vehicle control and incubated for 24 or 48 h. Subsequently, cells were detached, washed with PBS, and stained with fluochrome solution (50 μg/mL PI in a solution of 0.1 % sodium citrate (w/v) and 0.1 % Triton X-100 (v/v) in deionized water) for 30 min at 4 °C in the dark. Cell cycle was analyzed using a BD FACS Canto™ II and data were evaluated using FlowJo 7.6 software.

Cell Uptake Assay: The uptake of PBs was determined by analytical HPLC analysis. 1.5×10^6 T24 cells were seeded in 60 mm dishes and incubated for one day. Next, cells were treated with *Cj*-PleB (**1**), *Po*-PleB (**3**), PxB (**2**), and PleB-esters (**4–7**) (80 μM) for 5 h. After washing twice with ice-cold PBS, cells were scraped off in 500 μL of PBS and cell suspension was centrifuged at 13000 rpm for 5 min at 4 °C. The supernatant was discarded and the cell pellet was again washed with PBS. Cells were lysed by bead beating and proteins were precipitated with 120 μL of ACN/PBS (20:80) for 1 h on ice. Lysates were centrifuged again and a 50 μL aliquot of the supernatant was analyzed by HPLC. The peak areas of the different compounds were normalized to the peak area of the butylated ester, which was set to 100 %.

Statistical Analysis: Results represent the mean of at least three independent experiments (means ± standard deviation) performed in at least three replicates unless stated otherwise. Statistical significance was carried out by two-way analysis of variance with post hoc analysis using Dunnett's multiple comparison test; all statistical analyses were processed with GraphPad Prism 7.05.

Acknowledgments

[1] a) B. Kräutler, *Chem. Soc. Rev.*, **2014**, 43, 6227-6238; b) B. Kräutler, B. Jaun, K. Bortlik, M. Schellenberg, P. Matile, *Angew. Chem. Int. Ed. Engl.* **1991**, 30, 1315–1318; *Angew. Chem.* **1991**, 103, 1354.

[2] C. Curty, N. Engel, *Phytochemistry* **1996**, 42, 1531–1536.

[3] S. Moser, M. Ulrich, T. Müller, B. Kräutler, *Photochem. Photobiol. Sci.* **2008**, 7, 1577–1581.

[4] C. Vergeiner, M. Ulrich, C. Li, X. Liu, T. Müller, B. Kräutler, *Chem. Eur. J.* **2015**, 21, 136–149.

[5] C. J. Li, K. Wurst, S. Jockusch, K. Gruber, M. Podewitz, K. R. Liedl, B. Kräutler, *Angew. Chem. Int. Ed.* **2016**, 55, 15760–15765; *Angew. Chem.* **2016**, 128, 15992.

[6] S. Moser, B. Kräutler, *Isr. J. Chem.* **2019**, *59*, 420–431.

[7] C. A. Karg, P. Wang, A. M. Vollmar, S. Moser, *Phytomedicine* **2019**, *60*, 152969.

[8] C. Karg, C. Schilling, L. Allmendinger, S. Moser, *J. Porphyrins Phthalocyanines* **2019**, *23*, 881–888.

[9] P. Keshavan, S. J. Schwemberger, D. L. H. Smith, G. F. Abcock, S. D. Zucker, *Int. J. Cancer* **2004**, *112*, 433–445.

[10] M. Ulrich, S. Moser, T. Müller, B. Kräutler, *Chem. Eur. J.* **2011**, *17*, 2330–2334.

[11] K. L. Wüthrich, L. Bovet, P. E. Hunziker, I. S. Donnison, S. Hörtensteiner, *Plant J.* **2000**, *21*, 189–198 .

[12] a) B. Kräutler, *Angew. Chem. Int. Ed.* **2016**, *55*, 4882–4907; *Angew. Chem.* **2016**, *128*, 4964; b) M. Oberhuber, J. Berghold, K. Breuker, S. Hörtensteiner, B. Kräutler, *Proc. Natl. Acad. Sci. USA* **2003**, *100*, 6910–6915.

[13] D. Wakana, H. Kato, T. Momose, N. Sasaki, Y. Ozeki, Y. Goda, *Tetrahedron Lett.* **2014**, *55*, 2982–2985.

[14] M. Scherl, T. Müller, B. Kräutler, *Chem. Biodiversity* **2012**, *9*, 2605–2617.

[15] T. Erhart, C. Mittelberger, C. Vergeiner, G. Scherzer, B. Holzner, P. Robatscher, M. Oberhuber, B. Kräutler, *Chem. Biodiversity* **2016**, *13*, 1441–1453.

[16] M. Scherl, T. Müller, C. Kreutz, R. G. Huber, E. Zass, K. R. Liedl, B. Kräutler, *Chem. Eur. J.* **2016**, *22*, 9498–9503.

[17] B. Kuai, J. Chen, S. Hörtensteiner, *J. Exp. Bot.* **2017**, *69*, 751–767.

[18] J. Liu, H. Wang, N. E. Manicke, J.-M. Lin, R. G. Cooks, Z. Ouyang, *Anal. Chem.* **2010**, *82*, 2463–2471.

[19] J. Liu, H. Wang, R. G. Cooks, Z. Ouyang, *Anal. Chem.* **2011**, *83*, 7608–7613.

[20] B. Christ, M. Hauenstein, S. Hörtensteiner, *Plant J.* **2016**, *88*, 505–518.

[21] T. Müller, S. Vergeiner, B. Kräutler, *Int. J. Mass Spectrom.* **2014**, *365–366*, 48–55.

[22] A. Gossauer, *The Chemistry of Linear Oligopyrroles and Bile Pigments* (Ed.: H. Falk), Springer, Wien **1989**. XII, 621 pp., ISBN 3-211-82112-0. **1990**, 102 (3), 345–346. **1990**, *102*, 345–346.

[23] J. Y. Takemoto, C.-W. T. Chang, D. Chen, G. Hinton, *Isr. J. Chem.* **2019**, *59*, 378–386.

[24] S. Gazzin, L. Vitek, J. Watchko, S. M. Shapiro, C. Tiribelli, *Trends Mol. Med.* **2016**, *22*, 758–768.

[25] J. Kapitulnik, *Mol. Pharmacol.* **2004**, *66*, 773–779.

[26] P. Rao, R. Suzuki, S. Mizobuchi, T. Yamaguchi, S. Sasaguri, *Biochem. Biophys. Res. Commun.* **2006**, *342*, 1279–1283.

[27] T. Müller, M. Ulrich, K. H. Ongania, B. Krautler, *Angew. Chem. Int. Ed.* **2007**, *46*, 8699–8702; *Angew. Chem.* **2007**, *119*, 8854.

[28] a) I. Nicoletti, G. Migliorati, M. C. Pagliacci, F. Grignani, C. Riccardi, *J. Immunol. Methods* **1991**, *139*, 271–279; b) C. Riccardi, I. Nicoletti, *Nat. Protoc.* **2006**, *1*, 1458–1461.

[29] I. Süssenbacher, C. Kreutz, B. Christ, S. Hörtensteiner, B. Kräutler, *Chem. Eur. J.* **2015**, *21*, 11664–11670.

[30] S. Moser, T. Müller, M.-O. Ebert, S. Jockusch, N. J. Turro, B. Kräutler, *Angew. Chem. Int. Ed.* **2008**, *47*, 8954–8957; *Angew. Chem.* **2008**, *120*, 9087.

[31] T. Erhart, C. Mittelberger, X. Liu, M. Podewitz, C. Li, G. Scherzer, G. Stoll, J. Valls, P. Robatscher, K. R. Liedl, M. Oberhuber, B. Kräutler, *Chem. Eur. J.* **2018**, *24*, 17268–17279.

[32] M. Roca, A. Pérez-Gálvez, *J. Nat. Prod.* **2020**, *83*, 873–880.

[33] R. Zhang, X. Qin, F. Kong, P. Chen, G. Pan, *Drug Delivery* **2019**, *26*, 328–342.